JCTC Journal of Chemical Theory and Computation

Article

pubs.acs.org/JCTC

# Broad Transferability of Substituent Effects in π-Stacking Interactions Provides New Insights into Their Origin

Rajesh K. Raju, Jacob W. G. Bloom, and Steven E. Wheeler*

Department of Chemistry, Texas A&M University, College Station, Texas 77842, United States

Supporting Information

**ABSTRACT:** Substituent effects in model stacked homodimers and heterodimers of benzene, borazine, and 1,3,5-triazine have been examined computationally. We show that substituent effects in these dimers are strongly dependent on the identity of the unsubstituted ring, yet are independent of the ring bearing the substituent. This supports the local, direct interaction model [*J. Am. Chem. Soc.* **2011**, *133*, 10262], which maintains that substituent effects in π-stacking interactions are dominated by through-space interactions of the substituents with the proximal vertex of the unsubstituted ring. In addition to dimers in which the unsubstituted ring is held constant, substituent effects are correlated in many other stacked dimers, including those in which neither the substituted nor unsubstituted rings are conserved. Whether substituent effects in a pair of dimers will be correlated is shown to hinge on the electrostatic components of the interaction energies, and the correlations are explained in terms of the interaction of the local dipole moments associated with the substituents and the electric fields of the unsubstituted rings. Overall, substituent effects are similar in two stacked dimers as long as the electric fields above the unsubstituted rings are similar, providing a more sound physical justification for the local, direct interaction model.

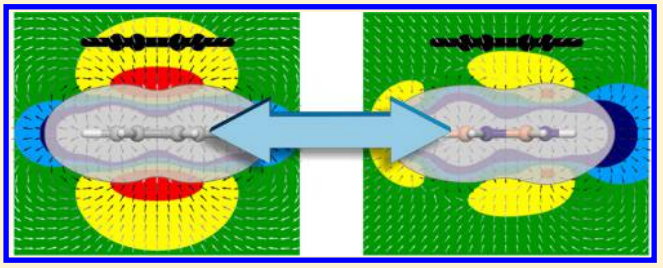

## I. INTRODUCTION

Noncovalent interactions involving aromatic rings pervade modern chemical research.[1−3] Among these, π-stacking interactions play pivotal roles in a myriad of phenomena ranging from protein−DNA interactions and supramolecular self-assembly to organocatalysis.[1−7] Substituents are often used to tune the strength of these interactions,[8] and further unraveling their physical origin will enable more-refined exploitation of substituent effects in chemical applications. For example, there has been increasing interest in harnessing the effects of heteroatoms and substituents to control the molecular packing of small molecule semiconductors for the development of high-performance organic electronic materials.[9,10] Similarly, we recently demonstrated[11] that through-space substituent effects in π-stacking interactions can be used to control the local orientation of model stacked discotic systems in order to maximize charge-transfer rates.

Computational studies of π-stacking interactions typically consider three prototypical configurations of the benzene dimer, depicted in Figure 1.[12] Among these, the sandwich dimer is the most extensively studied, despite this configuration being a saddle point on the potential energy surface.[13] The parallel-displaced and T-shaped dimers are roughly isoenergetic and are both energy minima. We recently demonstrated[14] that substituent effects in the benzene sandwich dimer are correlated with those in the parallel-displaced dimer, supporting the use of the more symmetric sandwich dimer as a model for unraveling substituent effects in π-stacking interactions.[8]

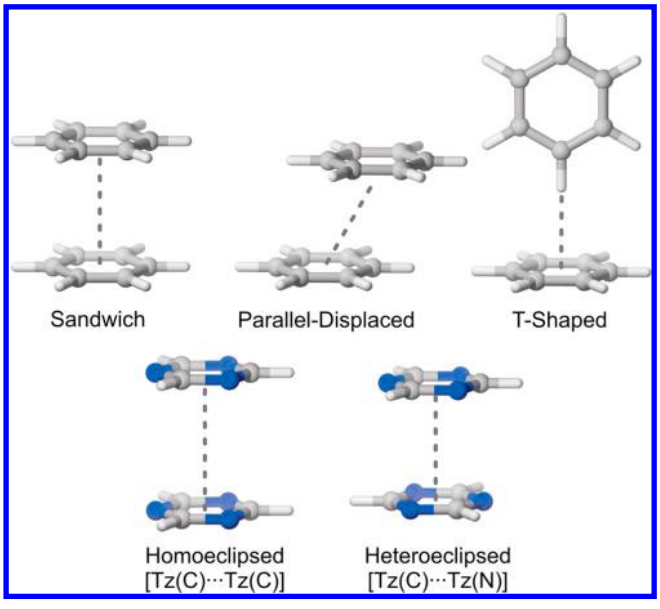


**Figure 1.** Prototypical benzene dimer configurations (top), as well as sandwich heteroeclipsed and homoeclipsed triazine dimers (bottom).

Substituent effects in π-stacking interactions have been discussed at length in recent years, and their origin is thought to be well understood.[8,14−17] Traditional conceptual models of

**Received:** June 7, 2013
**Published:** June 25, 2013

substituent effects in $\pi$-stacking interactions, including those of Hunter and co-workers[18−22] and Cozzi and Siegel,[23−28] were cast primarily in terms of substituent-induced changes in the aryl $\pi$-system. In recent years, however, accurate gas-phase computational studies[12,14,16,17,29−39] have pinpointed apparent flaws in these popular views.[18−28] While these conventional models posit that electron-accepting substituents enhance $\pi$-stacking interactions and donors hinder $\pi$-stacking, model gas-phase computations revealed that all substituents stabilize the benzene dimer relative to the unsubstituted case, regardless of their electron-withdrawing or electron-donating character.[9b,12a,12e,12i] However, in the case of monosubstituted sandwich dimers,[33] interaction energies for the substituted dimers remain correlated with Hammett $\sigma$ constants, with the unsubstituted dimer being an outlier. In other words, substituent effects in gas-phase benzene sandwich dimers follow the general trend predicted by conventional models of $\pi$-stacking,[18−28] but with the caveat that the substituted dimers exhibit enhanced stabilization in the gas phase, relative to the hydrogen case, because of dispersion effects.

In 2008, Wheeler and Houk demonstrated[33] that substituent effects in the sandwich configuration of the benzene dimer are due primarily to direct, through-space interactions between the substituents and the unsubstituted ring. Substituent-induced changes in the $\pi$-system of the substituted ring were shown not to contribute significantly. Such direct interactions had previously been invoked in an ad hoc manner by Rashkin and Waters[40] and Sherrill et al.[31,34] to explain unexpected substituent effects in parallel-displaced and T-shaped interactions.

More recently, we presented a new model[14] of substituent effects in $\pi$-stacking interactions in which substituent effects are dominated by local, direct interactions (i.e., field effects) between the substituents and the proximal vertex of the other ring. The essence of this model is that substituent effects are unchanged as long as no atomic substitutions are made within the local environment of the substituent (see Figure 2). The

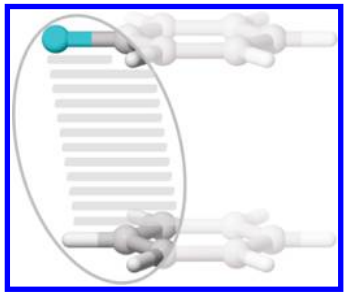

**Figure 2.** In the local, direct interaction model[14] of substituent effects in $\pi$-stacking interactions, substituent effects are predicted to be unchanged as long as the atoms present in the unshaded region remain unchanged.

presumed basis of this model was that substituent effects arise primarily from the electrostatic interaction between the local dipole associated with the substituent and the local C−H dipole in the proximal vertex of the unsubstituted ring. However, concrete evidence for this presumed origin was lacking.

One ramification of this model[14] is that substituent effects in $\pi$-stacking interactions are expected to be highly transferable. In other words, substituent effects will be independent of the nature of the aryl ring to which the substituent is attached; instead, they will depend on the identity of the atoms in the proximal vertex of the unsubstituted ring. Such transferability of substituent effects was demonstrated for homodimers and heterodimers of benzene and pyridine.[14] What remains unanswered, however, is to what extent changes can be made to both the substituted and unsubstituted ring without significantly altering substituent effects. In other words, under what circumstances will two stacked dimers exhibit the same substituent effects?

By probing the transferability of substituent effects in $\pi$-stacking interactions, we can gain new insight into the origin of these effects. Moreover, the transferability of substituent effects in aryl−aryl interactions is vital for the development of atomistic and coarse-grained molecular−mechanical force fields for applications to organic electronic materials. Such transferability would justify the development of general, transferable force fields for substituents that are independent of the arene to which the substituents are attached.

In the present work, we probe the transferability of substituent effects in $\pi$-stacking interactions by examining sandwich dimers involving benzene (Bz), borazine (Bn), and 1,3,5-triazine (Tz) (see Figure 3). These systems exhibit

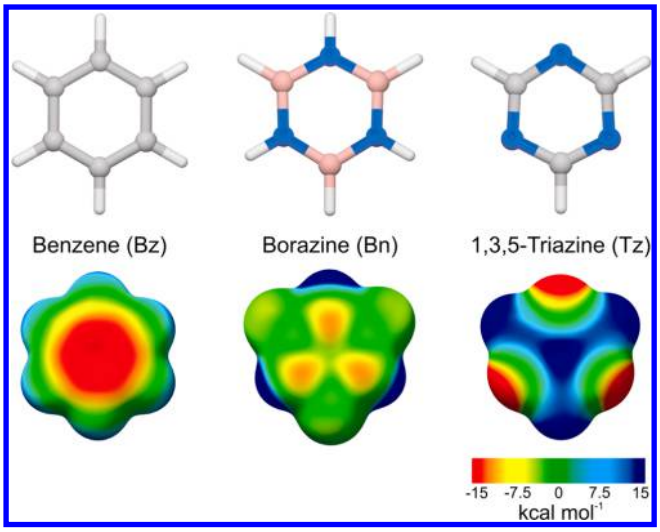


**Figure 3.** Structures and molecular electrostatic potentials (ESPs) of benzene, borazine, and triazine.

drastically different electronic character and provide a means of probing the transferability of substituent effects across diverse stacked systems. Moreover, all three of these systems are planar, yet exhibit varying degrees of aromaticity. Additionally, there has been growing interest in the use of B- and N-heterocycles in organic electronic materials,[41−48] in materials for gas-storage and separation,[49−56] and even as enzyme inhibitors.[57−60] All of these applications will benefit from refined control over $\pi$-stacking interactions involving N- and B-heterocycles.

Anand and co-workers[61] reported that many substituted borazines exhibit $\pi$-stacking interactions in the solid state, although, in some cases, other interactions dominate. There have been a limited number of computational studies[62,63] of $\pi$-stacking interactions involving borazine and no computational studies of substituent effects in these dimers. In 2003, Kawahara et al.[62] presented MP2 and CCSD(T) results for sandwich, parallel-displaced, and T-shaped borazine dimers, finding that the heteroeclipsed borazine sandwich dimer (see Figure 1 for analogous triazine dimer) was the most strongly interacting.

More recently, Bettinger et al.[63] studied homodimers and heterodimers of benzene and borazine.

There have been several computational studies[64−70] of stacked triazine dimers over the past decade, but, as with the borazine dimers, there have been no systematic studies of substituent effects. In 2005, Ugozzoli and Massera[64] examined stacked dimers of benzene and triazine, predicting a strong interaction between benzene and triazine in a parallel-displaced configuration. Three years later, Tschumper et al.[65] studied the effects of heterogeneity on $\pi$-stacking interactions, including those in parallel-displaced benzene and triazine homodimers and heterodimers. They found that, for the parallel-displaced dimers, the interaction energy in the mixed triazine−benzene dimer (−3.8 kcal mol$^{-1}$) was more favorable than that of homodimers of either benzene (−2.8 kcal mol$^{-1}$) or triazine (−3.0 kcal mol$^{-1}$). A correlation was reported between the electrostatic component of these interactions, as predicted by second-order symmetry-adapted perturbation theory (SAPT2), and the total interaction energies.[65] Also in 2008, Wang and Hobza studied[66] $\pi$-stacking interactions of several *N*-heterocycles with benzene. In contrast to Tschumper et al.,[65] they attributed the stronger interaction of triazine with benzene, relative to the benzene homodimer, to dispersion effects based on the higher polarizability of triazine. More recently, Mishra et al. studied[67] both stacking and edge-to-face interactions for a range of *N*-heterocyclic dimers, finding that the strength of these interactions were comparable. Kim and co-workers[68,69] employed both spectroscopic and computational techniques to study noncovalent interactions of phenylacetylene with triazine, pyrazine, and pyridine, reporting that parallel-displaced $\pi$-stacking configurations are preferentially formed over other arrangements. Finally, in 2012, Sütay et al. studied[70] various pyrazine and triazine homodimers using a range of computational methods, reporting that either parallel-displaced or hydrogen-bonded dimers are the most favorable, depending on the level of theory employed.

Below, we systematically study substituent effects in stacked homodimers and heterodimers of benzene, borazine, and triazine. The primary aim is to probe the extent to which substituent effects in $\pi$-stacking interactions are transferable among these diverse stacked systems. The results indicate that substituent effects do not depend on the ring to which the substituent is attached, but are instead determined by the identity of the unsubstituted ring. Moreover, unexpected correlations among substituent effects in disparate stacked dimers provide new insight into the origin of substituent effects in $\pi$-stacking interactions. These correlations are explained based on computed electric fields for the unsubstituted arenes, which supports the view that substituent effects in $\pi$-stacking interactions are dominated by the electrostatic interaction of the local dipole associated with the substituent and the other ring.

## II. THEORETICAL METHODS

Interaction energies for a wide range of eclipsed sandwich dimers were evaluated at the CCSD(T), SAPT0, and B97-D levels of theory.[71−80] For the unsubstituted dimers, counterpoise-corrected[81] CCSD(T)/AVTZ interaction energies were estimated by appending a basis set correction evaluated at the MP2 level onto CCSD(T)/AVDZ energies:

$$\text{CCSD(T)/AVTZ} \approx \text{CCSD(T)/AVDZ} + [\text{MP2/AVTZ} - \text{MP2/AVDZ}]$$

where AVXZ denotes the aug-cc-pVXZ basis set of Dunning and co-workers.[78,82] To locate the equilibrium inter-ring separation ($R_e$) for each dimer, a series of single point energies were evaluated at this level of theory at 0.1 Å increments near the minima. A simple quadratic function was fit to the 3−4 lowest-lying points to interpolate the $R_e$ value and interaction energy. These computations utilized fixed monomer geometries optimized at the MP2/AVTZ level of theory. To gain additional insight into the interaction of these nonsubstituted dimers, SAPT0 interaction energies[73−76] were evaluated at the CCSD(T) predicted equilibrium separations using the jun-cc-pVDZ basis set.[83] The jun-cc-pVDZ basis set comprises the standard Dunning aug-cc-pVDZ basis set, but without diffuse functions on hydrogen and without diffuse *f* functions on non-hydrogen atoms (i.e., the aug-cc-pVDZ′ used by Sherrill and co-workers[12,84]). SAPT predicts accurate intermolecular interaction energies, while also providing a rigorous decomposition of these interaction energies into physically meaningful components ($E_{int} = E_{elec} + E_{exch} + E_{ind} + E_{disp}$).

To examine the impact of substituents on these stacked dimers, we considered a diverse set of 22 substituents: $BF_2$, CCH, $CF_3$, $CH_2OH$, $CH_3$, CHO, CN, $COCH_3$, $COOCH_3$, COOH, F, $NH_2$, $NHCH_3$, $NO_2$, NO, $OCF_3$, OH, $OCH_3$, $SCH_3$, SH, $SiF_3$, and $SiH_3$. This set of substituents provides a representative sample, and ranges from strong electron donors (e.g., $NHCH_3$) to strong electron-acceptors (e.g., $NO_2$). For each substituted arene, monomers were optimized at the B97-D/TZV(2*p*,2*d*) level of theory.[77−80] For many substituents there are multiple low-lying rotamers. For substituted borazines and triazines, the substituent rotamer that is equivalent to the lowest lying rotamer for substituted benzene was used.

Geometries of all possible eclipsed monosubstituted sandwich dimers of benzene, borazine, and triazine (460 dimers total) were optimized with fixed monomer geometries at the B97-D/TZV(2*d*,2*p*) level of theory.[77−80] For the asymmetric substituents, the arene faces will be unique, so there are two ways of forming the stacked sandwich dimers. We determined the most favorable arrangement for the benzene dimer and replicated this orientation for the other dimers. This facilitated direct comparisons of substituent effects across the different substituted dimers. Given the relatively poor performance of B97-D for many of the unsubstituted dimers (vide infra), SAPT0/jun-cc-pVDZ interaction energies were computed for all substituted dimers at the B97-D optimized equilibrium separations. SAPT0 energies were also evaluated at inter-ring separations of 3.5 and 4.0 Å for all dimers.

Borazine and triazine have only 3-fold symmetry, and borazines can be substituted at either the boron or nitrogen positions. To distinguish among the different sites of substitution, and to denote which atoms are eclipsed in the stacked dimers, we have adopted the following naming scheme. Bn(N)-X and Bn(B)-X denote borazines substituted at the N and B sites, respectively. For dimers in which borazine is unsubstituted, Bn(N) and Bn(B) indicate that the substituted atom of the other ring is aligned with the N and B of borazine, respectively. Similarly, for dimers in which triazine is the unsubstituted ring, Tz(N) and Tz(C) indicate that the N and C−H of triazine are eclipsed with the substituted atom of the other ring, respectively (see later figures for examples).

Table 1. Estimated CCSD(T)/AVTZ and B97-D/TZV(2*d*,2*p*) Interaction Energies ($E_{int}$) and Equilibrium Inter-Ring Separations ($R_e$, in Å), SAPT0 Energy Components, and Total SAPT0 Interaction Energies ($E_{int}$) for Dimers of Benzene (Bz), Borazine (Bn), and Triazine (Tz)[a]

| | | CCSD(T) | | B97-D | | SAPT0//CCSD(T) | | | | | SAPT0//B97-D |
|---|---|---|---|---|---|---|---|---|---|---|---|
| | | $R_e$ | $E_{int}$ (kcal mol$^{-1}$) | $R_e$ | $E_{int}$ (kcal mol$^{-1}$) | $E_{elec}$ (kcal mol$^{-1}$) | $E_{exch}$ (kcal mol$^{-1}$) | $E_{ind}$ (kcal mol$^{-1}$) | $E_{disp}$ (kcal mol$^{-1}$) | $E_{int}$ (kcal mol$^{-1}$) | $E_{int}$ (kcal mol$^{-1}$) |
| Bz | Bz | 3.92 | −1.6 | 3.90 | −1.8 | 0.4 | 3.3 | −0.2 | −4.8 | −1.4 | −1.4 |
| | Bn | 3.79 | −2.2 | 3.69 | −3.1 | −0.6 | 3.6 | −0.3 | −4.6 | −1.9 | −1.9 |
| | Tz | 3.67 | −3.1 | 3.69 | −3.2 | −2.0 | 4.6 | −0.3 | −5.4 | −3.2 | −3.2 |
| Bn(B) | Bn(B) | 3.89 | −1.8 | 3.65 | −3.3 | 0.1 | 2.0 | −0.1 | −3.2 | −1.2 | −0.6 |
| | Bn(N) | 3.52 | −3.3 | 3.28 | −5.9 | −3.0 | 5.7 | −0.4 | −5.4 | −3.1 | −3.1 |
| | Tz(C) | 3.68 | −2.7 | 3.59 | −3.7 | −0.8 | 3.1 | −0.2 | −4.2 | −2.1 | −1.9 |
| Tz(C) | Bn(N) | 3.56 | −3.1 | 3.48 | −4.0 | −2.2 | 4.4 | −0.3 | −5.0 | −3.1 | −3.2 |
| | Tz(C) | 3.74 | −1.5 | 3.97 | −1.8 | 0.9 | 2.1 | −0.1 | −3.8 | −1.0 | −1.0 |
| | Tz(N) | 3.46 | −3.8 | 3.50 | −3.9 | −3.3 | 5.3 | −0.4 | −5.8 | −4.2 | −4.2 |

[a] $E_{elec}$ = electrostatic, $E_{exch}$ = exchange-repulsions, $E_{ind}$ = induction, and $E_{disp}$ = dispersion.

Throughout this work, A, B, C, etc. are used to denote any of Bz, Bn(N), Bn(B), Tz(C), or Tz(N).

Molecular electrostatic potential (ESP) maps (Figure 3) were created using UCSF Chimera[85] by mapping the electrostatic potential, computed at the B97/TZV(2*d*,2*p*) level of theory, onto an electron-density isosurface ($\rho$ = 0.001 $e$/bohr$^3$). B97/TZV(2*d*,2*p*) electrostatic potentials and electric fields were also computed in the plane bisecting benzene, borazine, and triazine. All DFT computations were carried out using Gaussian09,[86] while Molpro[87] was employed to evaluate MP2 and CCSD(T) energies. SAPT0 energies were computed using Psi4.[88] Throughout this work, slopes between two sets of interaction energies were analyzed in terms of total least-squares (orthogonal regression), rather than the more common ordinary linear least-squares. Such analyses are more appropriate in this case, because the objective is to describe the linear correlation between two equivalent sets of data.

## III. RESULTS AND DISCUSSION

**A. Unsubstituted Dimers of Benzene, Borazine, and Triazine.** First, we consider unsubstituted sandwich dimers of benzene, borazine, and triazine. This will provide a baseline against which substituent effects can be compared, and will enable us to gauge the accuracy of B97-D and SAPT0 for these stacked dimers. Table 1 shows estimated CCSD(T)/AVTZ interaction energies for all unique sandwich dimers involving these three arenes. Heterodimers of triazine and borazine with benzene interact more strongly than the benzene homodimer, as previously noted;[63,65] the strongest interactions are predicted for heteroeclipsed borazine and triazine homodimers. That is, Bn(B)···Bn(N) interacts more strongly than Bn(B)···Bn(B) or the dimers of borazine with either triazine or benzene. The most favorable sandwich dimer is Tz(C)···Tz(N). The Tz(C)···Tz(N) sandwich dimer is more favorable than the parallel displaced configuration, as previously noted by Fowler and Buckingham[89] based on distributed multipole analyses and as predicted by venerable rules for aromatic interactions from Hunter and Sanders.[18] The data in Table 1 also underscore our previous finding that monomer aromaticity is not a prerequisite for strong stacking interactions.[90] For example, borazine is typically considered to be significantly less aromatic than benzene,[63,91] yet borazine stacks at least as strongly as benzene.

The origin of the observed trends in interaction energies are clarified by the SAPT0 components listed in Table 1. The electrostatic component of the interaction energies correlate strongly (correlation coefficient of $r$ = 0.95) with the total CCSD(T) interaction energies. The other SAPT0 components are also correlated with the total interaction energy, but this presumably is due to the coupling of effects through the interaction distance (as observed recently for XH/$\pi$ interactions).[92] Comparing Bn(B)···Bn(B) with Bn(B)···Bn(N), for example, the electrostatic component is strongly favorable for the more stable heteroeclipsed dimer, yet mildly unfavorable for the homoeclipsed dimer. This follows the findings of Tschumper and co-workers[65] regarding the impact of heterogeneity on $\pi$-stacking interactions.

Overall, the total SAPT0 interaction energies are strongly correlated with the reference CCSD(T) data ($r$ = 0.97), although SAPT0 generally underestimates the CCSD(T) interaction energies. On the other hand, the agreement between the B97-D/TZV(2*d*,2*p*) interaction energies and the CCSD(T) data is rather poor. In particular, B97-D overestimates the interaction energies, relative to CCSD(T), by anywhere from 2% to 85%. However, SAPT0 energies evaluated at the B97-D optimized structures are in agreement with the CCSD(T) data, with the exception of Bn(B)···Bn(B). Consequently, SAPT0 interaction energies for the substituted dimers are considered below for the substituted dimers.

**B. Substituent Effects in Sandwich Dimers of Benzene, Borazine, and Triazine.** Next, we consider the impact of substituents on the 20 possible sandwich dimers of benzene, borazine, and triazine. As noted above, substituent effects in most of these dimers have not previously been examined. The range of interaction energies for each dimer is plotted in Figure 4, along with interaction energies for X = H, CN, and $NH_2$ (see the Supporting Information (SI) for data). For many of the dimers, substituents enhance the strength of the interaction regardless of their electron-withdrawing or electron-donating character (i.e., X = H leads to the weakest interaction), in accord with previous observations for the benzene sandwich dimer.[16,29,33,37] However, in general, substituents lead to both enhanced and diminished $\pi$-stacking interactions, relative to the unsubstituted case. That is, for many of these dimers, the unsubstituted case (X = H) is not the

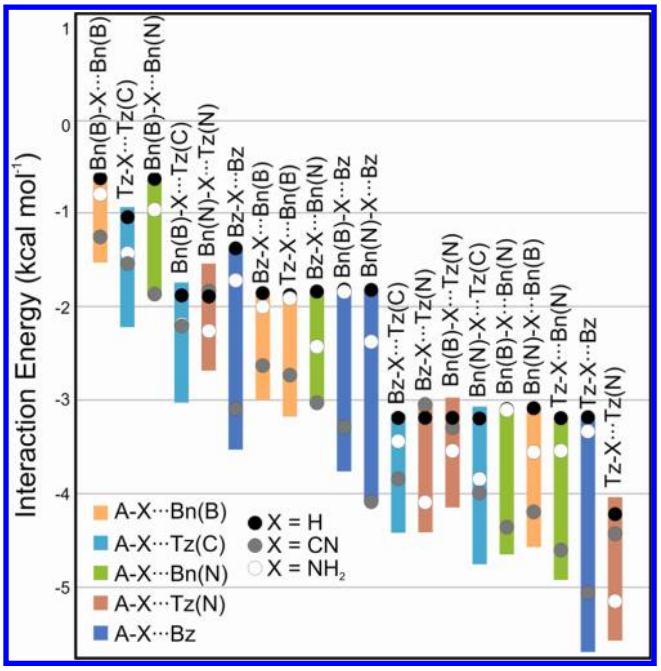


**Figure 4.** Span of interaction energies for substituted sandwich dimers of benzene, borazine, and triazine (filled rectangles), along with interaction energies for selected substituents (circles).

weakest interacting. Moreover, in many of these dimers, the substituent effects follow drastically different trends than in the benzene dimer. For example, in the benzene sandwich dimer, CN leads to strongly enhanced interactions relative to X = H, while $NH_2$ substituents provide only modest stabilization. This reflects differences in the electrostatic contributions to the interactions, which are highly favorable for X = CN, but not for X = $NH_2$. This can be contrasted with the A–X···Tz(N) dimers. In these cases, the impact of CN substituents is very weak, while X = $NH_2$ leads to substantial stabilization compared to X = H. This again reflects the underlying electrostatic component of these interactions: X = $NH_2$ leads to significant favorable electrostatic interactions, while CN substitution results in electrostatic interactions that are slightly less favorable than for X = H.

Overall, substituent and heteroatom effects provide powerful means of tuning the strength of $\pi$-stacking interactions, and the predicted interaction energies range from −0.6 kcal $mol^{-1}$ for the Bn(N)–H···Bn(N) dimer to −5.70 kcal $mol^{-1}$ for the Tz-$NO_2$···Bz dimer. Perhaps more importantly, as shown below, the impact of substituents and heteroatoms for a given unsubstituted ring are largely independent of each other, providing nearly orthogonal means of tuning the strength of $\pi$-stacking interactions.

**C. Transferability of Substituent Effects.** Next, we compare substituent effect trends across heterodimers and homodimers of benzene, borazine, and triazine. In Figure 5a, we see that substituent effects in Bz-X···Tz(C) dimers are completely uncorrelated with those in Bz-X···Tz(N) dimers ($r$ = 0.04). That is, rotating triazine by 60° completely alters the substituent effects in substituted benzene–triazine dimers. This behavior is observed in general; regardless of the identity of the substituted ring, changing the unsubstituted ring from Tz(C) to Tz(N) drastically alters the impact of substituents. This seems to be in conflict with expectations based on resonance-based views of substituent effects in $\pi$-stacking interactions. For

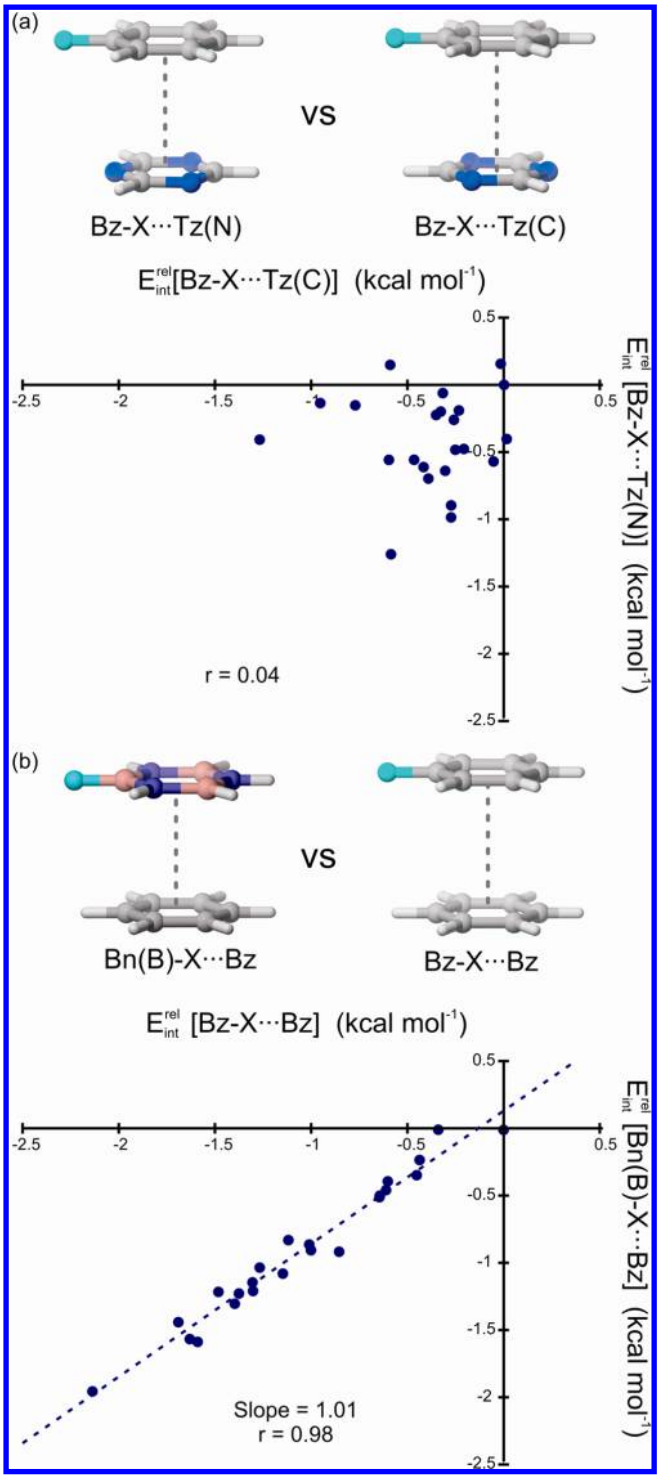


**Figure 5.** Relative SAPT0 interaction energies (kcal $mol^{-1}$) for sandwich dimers of (a) Bz–X···Tz(C) versus Bz–X···Tz(N) and (b) Bz–X···Bz versus Bn(N)–X···Bz.

example, in popular models,[18−22] substituent effects should depend only on the overall electron-rich or electron-poor character of the interacting rings, which is clearly independent of their relative orientation. Similarly, in the polar/$\pi$ model of Cozzi and Siegel,[23−28] substituent effects should be unaltered as long as the quadrupole moment of the unsubstituted ring remains constant. Instead, we see that aligning either the C–H or nitrogen vertex of triazine with the substituent on the other ring leads to drastically different substituent effects. Because of


dx.doi.org/10.1021/ct400481r | J. Chem. Theory Comput. 2013, 9, 3479−3490

the symmetry of triazine, molecular quadrupole moments alone do not distinguish between the two types of vertices, and any substituent effect model cast in terms of quadrupole moments will be unable to predict the lack of correlation in Figure 5a.

Figure 5a can be contrasted with Figure 5b, in which relative interaction energies for Bn(B)−X···Bz dimers are plotted against those for Bz−X···Bz. Despite the different electronic character of the substituted Bn(B) and Bz rings, we see a strong linear correlation ($r$ = 0.98) between substituent effects in these two dimers, with a best-fit line with slope near unity. Correlation coefficients and the slopes of total least-squares lines for all possible pairs of dimers of the type B−X···A vs A−X···A are listed in Table 2. For any pair of dimers for which the unsubstituted ring is the same, substituents effects are correlated (0.86 < $r$ < 0.98). That is, substituent effects in $\pi$-stacking interactions are dictated by the identity of the unsubstituted ring, with the substituted ring having no direct impact.[93]

**Table 2. Slopes and Correlation Coefficients ($r$) for Total Least Squares Analyses of SAPT0 Interaction Energies for Substituted Dimers of the Type B−X···A vs A−X···A**

| | | R = 3.5 Å | | R = $R_e$ | | R = 4.0 Å | |
|---|---|---|---|---|---|---|---|
| A | B−X | slope | r | slope | r | slope | r |
| Bz | Bn(B)−X | 0.94 | 0.96 | 1.01 | 0.98 | 0.96 | 0.98 |
| | Bn(N)−X | 1.05 | 0.98 | 1.10 | 0.98 | 1.01 | 0.98 |
| | Tz(C)−X | 1.03 | 0.96 | 1.18 | 0.98 | 1.04 | 0.96 |
| Bn(B) | Bz−X | 1.40 | 0.93 | 1.34 | 0.95 | 1.14 | 0.98 |
| | Bn(N)−X | 1.08 | 0.95 | 1.54 | 0.89 | 1.03 | 0.97 |
| | Tz(C)−X | 1.29 | 0.94 | 1.34 | 0.95 | 1.21 | 0.97 |
| Bn(N) | Bz−X | 0.85 | 0.87 | 0.95 | 0.86 | 0.85 | 0.96 |
| | Bn(B)−X | 0.84 | 0.91 | 1.39 | 0.92 | 0.92 | 0.94 |
| | Tz(C)−X | 0.88 | 0.91 | 1.30 | 0.94 | 0.99 | 0.91 |
| Tz(C) | Bz−X | 0.91 | 0.92 | 1.05 | 0.97 | 0.92 | 0.94 |
| | Bn(B)−X | 0.99 | 0.94 | 1.08 | 0.97 | 1.00 | 0.94 |
| | Bn(N)−X | 1.01 | 0.94 | 1.47 | 0.95 | 0.99 | 0.94 |

The deviations from unity of the best-fit line slopes in Table 2 arise in many cases from differences in the equilibrium inter-ring separations among the different sandwich dimers. For example, substituent effects in the Tz−X···Bz dimers are, on average, greater than those in the Bz−X···Bz dimers, because of the smaller average inter-ring separation for benzene−triazine heterodimers, compared to benzene homodimers. In this and many other cases, evaluating interaction energies at fixed inter-ring separations of either 3.5 Å or 4.0 Å ameliorates this problem to a large extent, leading to generally stronger correlations and slopes closer to unity (see Table 2).

Curiously, for some of the dimer pairs, evaluating the interaction energy at fixed inter-ring separations leads to best-fit lines with slopes slightly farther from one. For example, the slopes of the best-fit line is close to unity when comparing Bz−X···Bn(N) versus Bn(N)−X···Bn(N) at their corresponding $R_e$ values, yet deviate from one when evaluating interaction energies at inter-ring separations of either 3.5 or 4.0 Å. This potentially arises from differences in the ring geometries and the lengths of the bonds connecting the substituents with the rings, both of which affect the position of the substituent relative to the unsubstituted ring, despite the fixed inter-ring separation. Regardless, the overall trend is clear: as long as the unsubstituted dimer remains unchanged, substituent effect trends are transferable, even if the strength of the substituent effects shows some slight variability.

To quantify the extent of transferability of individual contributions to the interaction energies, we have also considered correlations among individual components of the SAPT0 interaction energies (see Table S2 in the SI). Comparing dimers of the type A−X···A with B−X···A, the data show that the electrostatic and dispersion components are each correlated. The correlations for the exchange components are slightly weaker. The induction components, which are admittedly small, show very weak (or even negative) correlations for many of the pairs of dimers. Nevertheless, the primary components of these interaction energies (electrostatic, dispersion, and exchange-repulsion effects) are all individually transferable among dimers in which the unsubstituted ring is held constant. This transferability of the individual components of these interaction energies is much stronger at fixed inter-ring separations, and justifies the

**Table 3. Slopes and Correlation Coefficients ($r$) for Total Least-Squares Analyses of SAPT0 Interaction Energies for A−X···B vs C−X···D Dimers, where A, B, C, and D are Bz, Bn(N), Bn(B), Tz(C), or Tz(N)[a]**

| | | Bz−X | | Bn(B)−X | | Bn(N)−X | | Tz−X | |
|---|---|---|---|---|---|---|---|---|---|
| B | A−X | slope | $r$ | slope | $r$ | slope | $r$ | slope | $r$ |
| | | | | C−X···Bn(N) | | | | | |
| Bz | Bz−X | 0.45 | 0.74 | 0.75 | 0.92 | 0.55 | 0.93 | 0.72 | 0.94 |
| | Bn(B)−X | 0.44 | 0.70 | 0.75 | 0.93 | 0.53 | 0.90 | 0.71 | 0.92 |
| | Bn(N)−X | 0.41 | 0.75 | 0.68 | 0.89 | 0.51 | 0.96 | 0.65 | 0.93 |
| | Tz−X | 0.35 | 0.67 | 0.62 | 0.89 | 0.44 | 0.88 | 0.60 | 0.92 |
| | | | | C−X···Bn(B) | | | | | |
| Bz | Bz−X | 0.58 | 0.90 | 0.43 | 0.90 | 0.64 | 0.86 | 0.59 | 0.95 |
| | Bn(B)−X | 0.57 | 0.90 | 0.43 | 0.92 | 0.62 | 0.81 | 0.59 | 0.95 |
| | Bn(N)−X | 0.52 | 0.87 | 0.38 | 0.88 | 0.58 | 0.87 | 0.53 | 0.93 |
| | Tz−X | 0.47 | 0.86 | 0.35 | 0.87 | 0.52 | 0.82 | 0.50 | 0.94 |
| | | | | C−X···Bn(N) | | | | | |
| Bn(B) | Bz−X | 0.84 | 0.61 | 1.33 | 0.84 | 0.92 | 0.83 | 1.25 | 0.81 |
| | Bn(B)−X | 1.28 | 0.67 | 1.82 | 0.84 | 1.28 | 0.85 | 1.70 | 0.85 |
| | Bn(N)−X | 0.71 | 0.62 | 1.18 | 0.76 | 0.81 | 0.83 | 1.10 | 0.80 |
| | Tz−X | 0.85 | 0.67 | 1.31 | 0.89 | 0.93 | 0.88 | 1.23 | 0.89 |

[a]SAPT0 interaction energies evaluated at B97-D/TZV(2d,2p) optimized dimer geometries.

development of classical potentials for substituents that are independent of the nature of the ring to which they are attached.

We also considered possible correlations between all pairs of dimers. Unexpectedly, in addition to the cases listed in Table 2, there are many pairs of dimers for which substituent effects are similar. In general, substituent effects are correlated between any two dimers in which the unsubstituted ring is Bz, Bn(N), or Bn(B), regardless of the identity of the substituted ring (see Table 3). For example, relative interaction energies for Tz−X···Bn(N) dimers are plotted against Bn(B)−X···Bz in Figure 6a. Substituent effects in these dimers are correlated ($r$ = 0.92), despite none of the rings being in common between the two dimers. Despite the correlations displayed in Table 3, the slopes of the best-fit lines deviate from one. This is particularly pronounced when comparing A−X···Bz dimers with either C−X···Bn(N) or C−X···Bn(B) dimers, for which substituent effects in the former case are consistently about twice as strong as those in the latter two dimers. These trends are also present for fixed inter-ring distances of 3.5 and 4.0 Å, and are not simply the result of cancellation of effects occurring at equilibrium distances (see Table S3 in the SI for data at $R$ = 3.5 and 4.0 Å). Instead, these correlations arise from some intrinsic similarity of benzene and borazine (vide infra). For all other dimers, linear correlations are weak or nonexistent, apart from a few aberrant cases (see Table S4 in the SI for full correlation matrix). Apparently, substituent effects in $\pi$-stacking interactions are not only transferrable in cases in which the unsubstituted ring remains constant, but also in select cases in which the substituted rings differ markedly in electronic character.

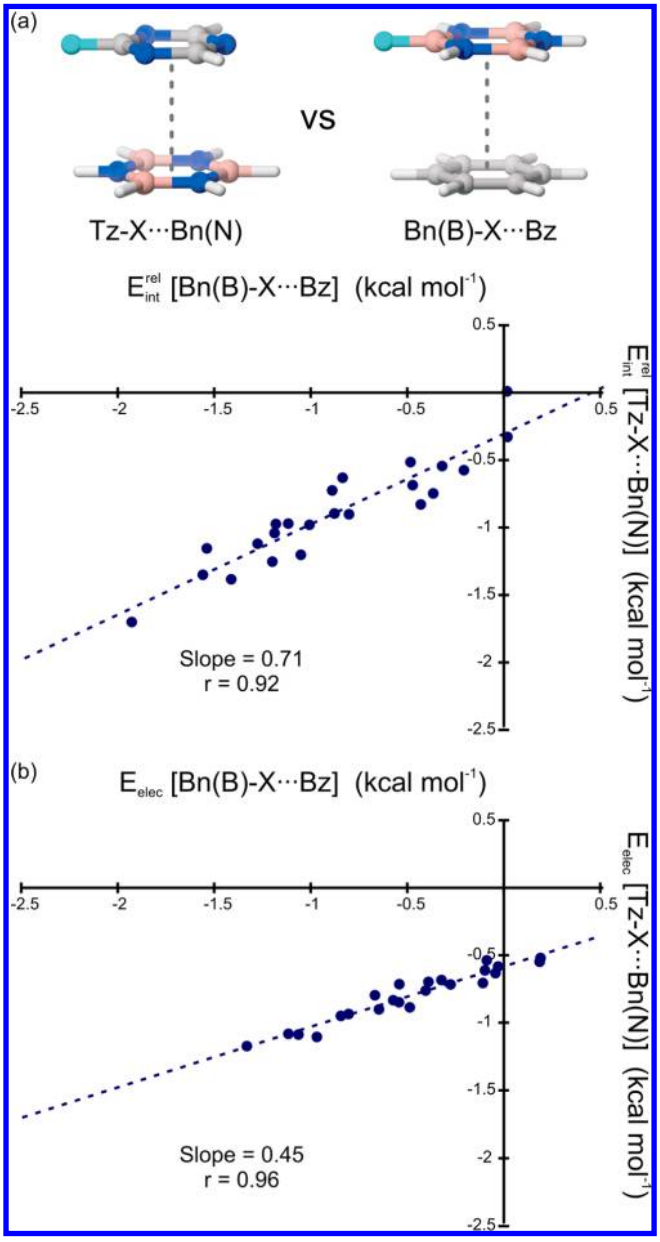


**Figure 6.** (a) Relative SAPT0 interaction energies ($R$ = $R_e$) and (b) electrostatic components of the interaction energies ($R$ = 4.0 Å) for sandwich dimers of Bn(B)−X···Bz versus Tz−X···Bn(N).

We again consider correlations of the individual components of the interaction energies, this time to determine which components of these interactions control whether substituent effects are correlated between two dimers. This was done at an inter-ring separation of 4.0 Å, to remove complications from varying inter-ring separations. The nonelectrostatic component of the SAPT0 interaction energies (i.e., $E_{nonelec} = E_{exch} + E_{ind} + E_{disp}$) is very strongly correlated between *all pairs of dimers* (see Figure 7a, for example, and Table S7 in the SI). That is, the impact of substituents on the nonelectrostatic part of the interaction energy is the same, regardless of the identity of the substituted or unsubstituted ring. As a result, whether two dimers will exhibit the same substituent effects hinges entirely on electrostatic effects. For pairs of dimers for which the electrostatic components are correlated, the total interaction energies are also correlated. In particular, the electrostatic components of the SAPT0 interaction energies are strongly correlated for all dimers in which the unsubstituted rings are Bz, Bn(N), or Bn(B). Moreover, the slopes of the best-fit lines are close to one-half when comparing the electrostatic components of the interaction energies in A−X···Bn(N) and A−X···Bn(B) dimers with B−X···Bz dimers, indicating that the electrostatic effects in the former two dimers are about half the strength of those in B−X···Bz dimers (e.g., see Figure 6b). This explains the nonunit slopes in Table 3.

Similarly, for pairs of dimers that exhibit uncorrelated electrostatic interactions, the total interactions are also uncorrelated. For example, Figure 7b shows the electrostatic components of the interaction energies of Bz−X···Tz(C) versus Bz−X···Tz(N) dimers. The lack of correlation between the total interaction energies (Figure 5a) stems primarily from the scatter in the electrostatic components of the interaction energies. In this and other cases, the electrostatic interactions are, to some extent, anticorrelated between the two dimers. Consequently, the total interaction energies are uncorrelated, because of the correlated nonelectrostatic components and anticorrelated electrostatic components.

That the correlation of substituent effects between two dimers depend solely on the electrostatic components of the interaction energies provides a physical justification for the local, direct interaction model of substituent effects in $\pi$-stacking interactions.[14] In particular, it corroborates the supposition that substituent effects derive from the electrostatic interaction of the local multipole (dominated by the local dipole) associated with the substituent with the other ring. To understand why these electrostatic interactions are similar in seemingly disparate dimers, we need to examine the electric fields of the unsubstituted arenes.


dx.doi.org/10.1021/ct400481r | J. Chem. Theory Comput. 2013, 9, 3479−3490

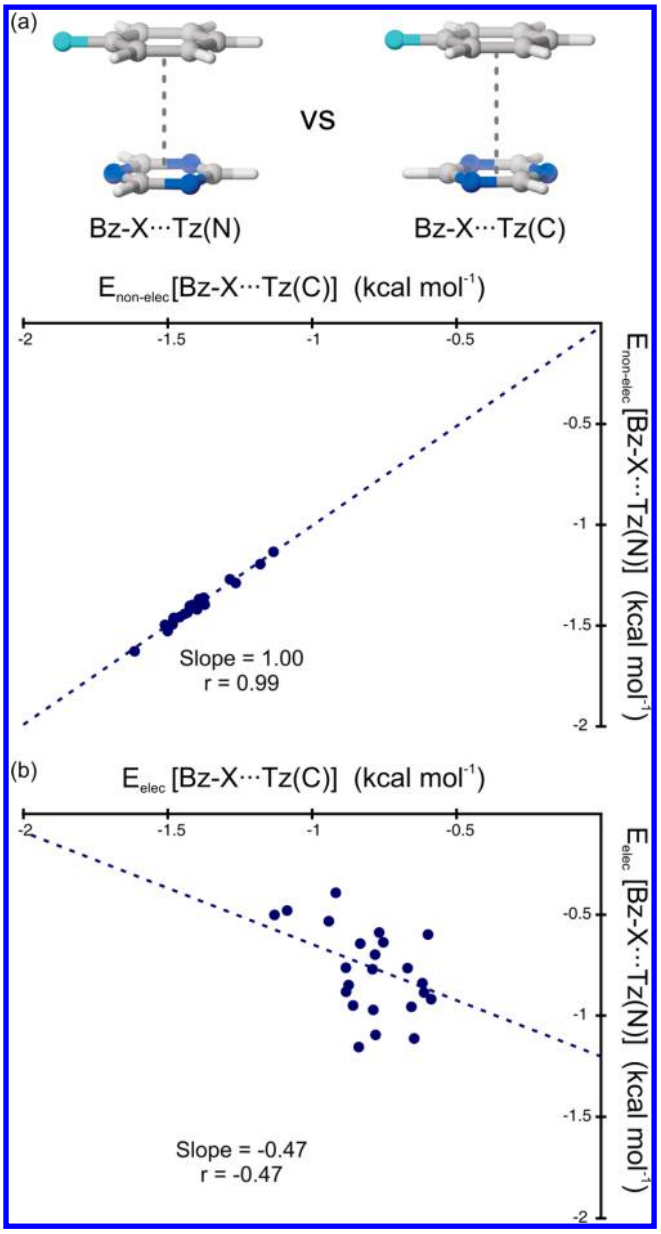


**Figure 7.** (a) Nonelectrostatic and (b) electrostatic components of the interaction energies for sandwich dimers of Bz−X···Tz(N) versus Bz−X···Tz(C), at $R$ = 4.0 Å.

**D. Substituent Effects and Electric Fields.** The electrostatic interaction of a dipole with a molecule depends on the dot product of the dipole with the molecular electric field. In Figure 8, electric fields in the plane perpendicular to the molecular planes and bisecting the rings are plotted for benzene, borazine, and triazine. Also plotted are the electrostatic potentials in this plane, for reference. In the region of the substituents, the electric field above both ends of borazine is similar in direction, but about half the magnitude, to that of benzene. The similarity of electric field direction above borazine and benzene can be seen in Figure 9a, in which we plot the dot product of the normalized electric field surrounding borazine with the electric field of benzene at each point. The strength of the borazine electric field, relative to that of benzene, is plotted in Figure 9b. Hence, the local dipole of the substituents will result in similar electrostatic interactions with either vertex of borazine as it will with

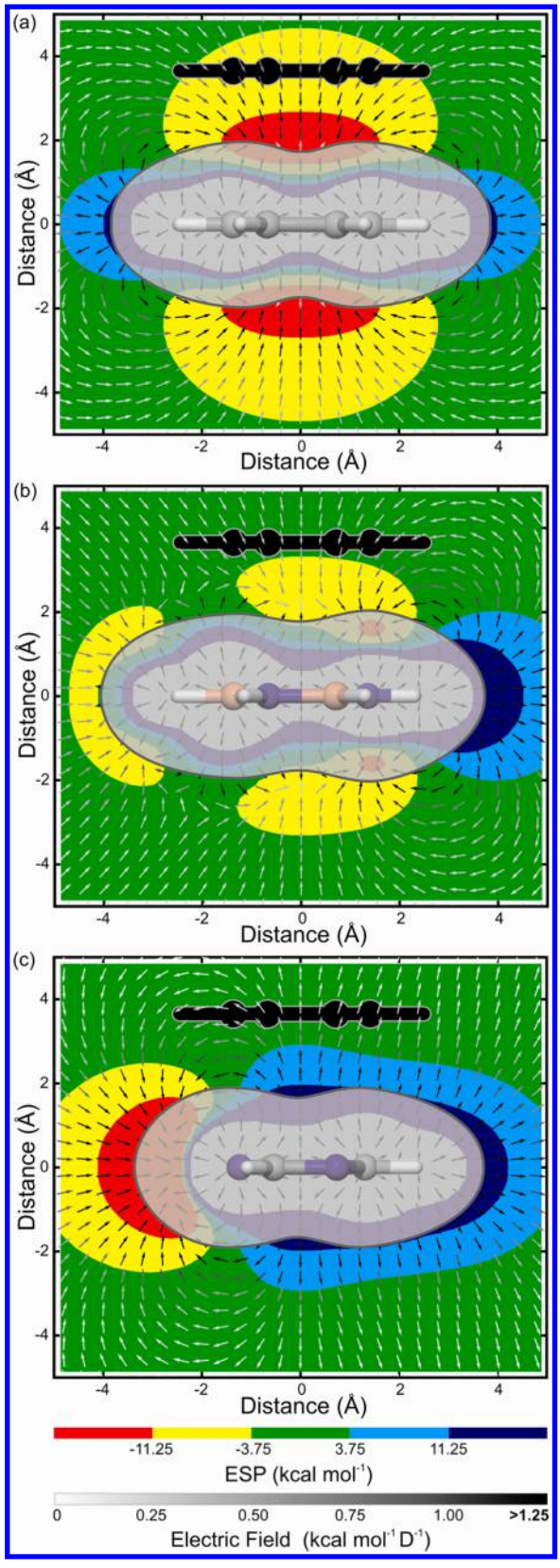


**Figure 8.** Electrostatic potential (solid colors, kcal mol$^{-1}$) and electric field (arrows, kcal mol$^{-1}$ D$^{-1}$) in the plane perpendicular to and bisecting the molecular plane of (a) benzene, (b) borazine, and (c) triazine. For reference, the gray-shaded region is an electron density isosurface ($\rho$ = 0.001 $e$/bohr$^3$) and the black silhouette is of a sandwich stacked benzene at $R$ = 3.65 Å.


dx.doi.org/10.1021/ct400481r | J. Chem. Theory Comput. 2013, 9, 3479−3490

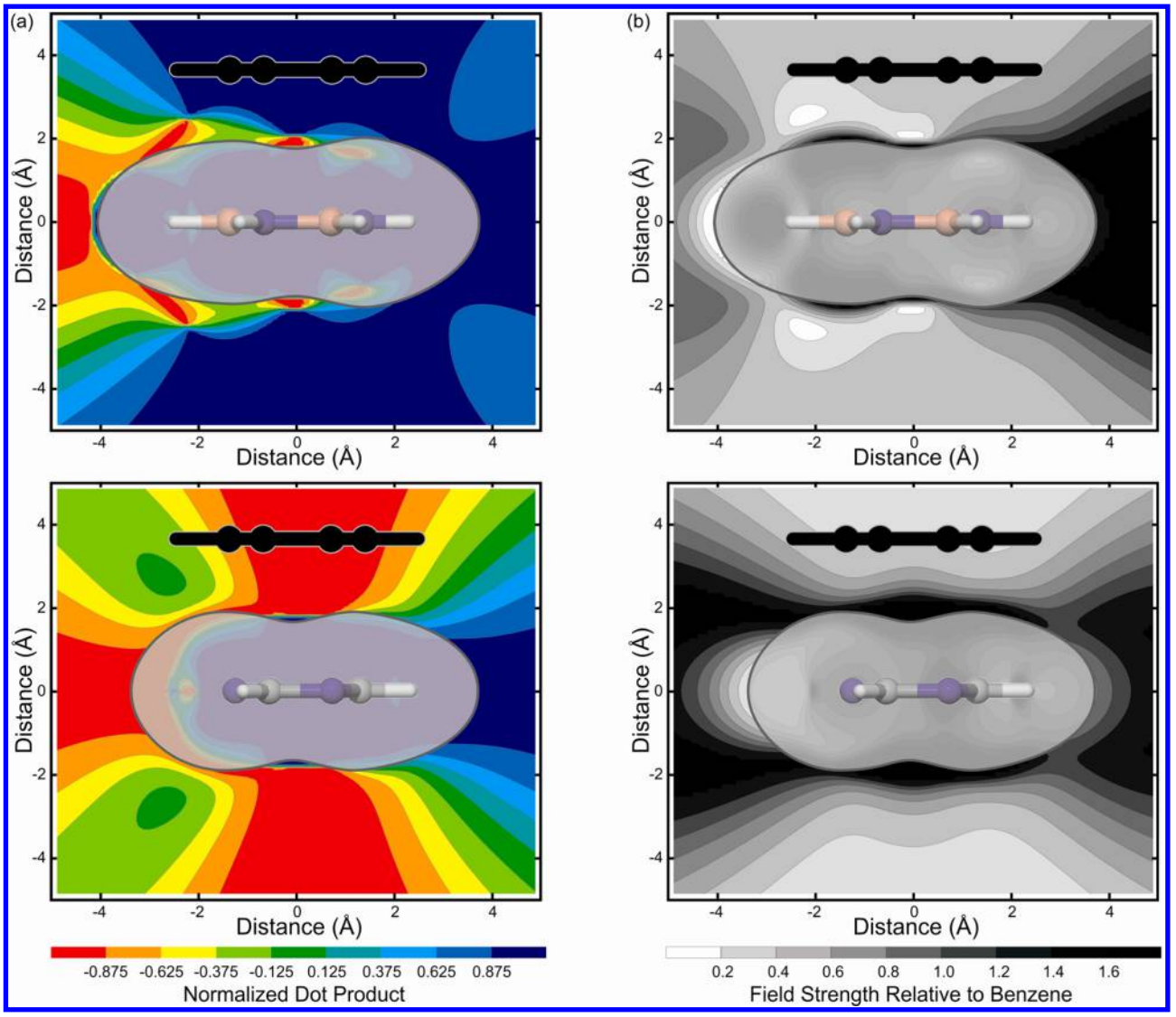


**Figure 9.** (a) Dot product of normalized electric field vectors of benzene with those of borazine (top) and triazine (bottom). In these plots, blue indicates the electric field is aligned with that of benzene, while red signifies anti-alignment. Green indicates that the electric field is orthogonal to that of benzene. (b) Strength of the electric field for borazine (top) and triazine (bottom) relative to the electric field of benzene. In both (a) and (b), the gray-shaded region is an electron density isosurface ($\rho$ = 0.001 $e$/bohr$^3$) and the black silhouette is of a sandwich stacked benzene at $R$ = 3.65 Å.

benzene, yet with about half the strength. This is in accord with the electrostatic data (see Figure 6b, for example), which showed that the electrostratic component of the substituent effects in A–X···Bn(N) dimers is about half that of B–X···Bz dimers. In other words, the correlation of substituent effects in A–X···Bn(N) and A–X···Bn(B) dimers with those in B–X···Bz dimers arises because the electric fields above the vertices of Bz, Bn(N), and Bn(B) are similar in direction. The nonunit slopes arise from the differences in the strengths of the electric fields.

This can be contrasted with the electric fields above either vertex of triazine. In these cases, the electric field is nearly orthogonal to that above benzene. Again, this can be seen in Figure 9a, which shows that in the region of the substituents the component of the triazine electric field along the benzene electric field is near zero. Thus, triazine and benzene will interact with different components of the local dipole associated with the substituent, giving rise to qualitatively different substituent trends. This explains the seemingly odd effects of $NH_2$ and CN substituents discussed in Section B. In particular, for A–X···Tz(N) dimers, X = $NH_2$ leads to highly favorable electrostatic interactions while, for X = CN, the electrostatic interactions are less favorable than in the unsubstituted dimers. This is in stark contrast to dimers in which benzene is the unsubstituted ring. The local dipole of CN is aligned with the electric field above benzene, while it is perpendicular to the field above triazine. Similarly, the local dipole of $NH_2$ is more closely aligned with the electric field of triazine than that of benzene.

Of course, the electric field is simply the negative gradient of the electrostatic potential, so the electric fields plotted in Figure 8 are obtainable visually, although indirectly, from electrostatic potential plots themselves. The key, however, is not to consider the sign of the ESP, but to focus on the *gradient of the ESP* in the region of the substituent. In this context, the customary practice of plotting ESPs on electron density isosurfaces (e.g., Figure 3) will generally not be helpful, as the electric field at points on these surfaces are not always representative of the electric field in the region of a substituent on a stacked ring.


dx.doi.org/10.1021/ct400481r | J. Chem. Theory Comput. 2013, 9, 3479–3490

Two-dimensional plots of the ESP more readily provide information about the ESP, and, indirectly, the electric field, in the proximity of the substituent.

In summary, the previously published local, direct interaction model (Figure 2)[14] is a special case for the transferability of substituent effects in $\pi$-stacking interactions. In addition to cases in which the atoms in the local environment of the substituent are unchanged, substituent effects will remain unaltered as long as changes to the unsubstituted ring *do not significantly alter the electric field surrounding the unsubstituted ring*. Unfortunately, such cases cannot be determined simply by examining the identity of the atoms in the local environment of the substituent (as indicated in Figure 2), but instead require examinations of computed electric fields (or ESPs). Once these fields have been computed for a set of unsubstituted arenes, they can be used to qualitatively determine substituent effects for the corresponding dimers. Regardless, the transferability of substituent effects among diverse stacked dimers can be explained based on the interaction of the local dipole moment associated with the substituent and the electric field of the unsubstituted arene. This provides significant new insight into the origin of substituent effects in $\pi$-stacking interactions, and emphasizes that electric fields can prove valuable in analyses of many noncovalent interactions in which local dipole moments are prevalent. Finally, we note that the electric fields displayed in Figure 8 are in a single plane bisecting the aryl rings. However, many substituents will have local dipoles located out of this plane, and the overall substituent effect will also depend on the electric field in these regions.

## IV. SUMMARY AND CONCLUDING REMARKS

We have presented gas-phase interaction energies for substituted homodimers and heterodimers of benzene, borazine, and triazine computed primarily at the SAPT0/jun-cc-pVDZ level of theory. Four main conclusions can be drawn from the data:

(1) Generally, the interaction energies of stacked sandwich dimers can be both enhanced or diminished by substituents, and for many dimers the substituent effects exhibit trends markedly different from those in the benzene sandwich dimer. Whether a given substituent leads to strongly enhanced stacking interactions does not depend on its electron-donating or electron-accepting character, but instead depends on the orientation of its local dipole moment, relative to the electric field of the unsubstituted ring.

(2) Substituent effects in $\pi$-stacking interactions are broadly transferable, and remain unchanged as long as the electric field of the unsubstituted ring in the vicinity of the substituent is unchanged. A special case of this occurs when the identity of the unsubstituted ring remains unchanged (i.e., the local, direct interaction model depicted in Figure 2).[14]

(3) The transferability of substituent effects in $\pi$-stacking interactions extends to the main components of these interactions (electrostatic, dispersion, and exchange-repulsion effects), which portends the development of molecular mechanics force fields that will accurately capture substituent effects in $\pi$-stacking interactions.

(4) Whether substituent effects are correlated between two dimers hinges entirely on the electrostatic components of the interactions. This supports the concept that substituent effects in $\pi$-stacking arise from the electrostatic interaction of the local dipole associated with the substituent and the electric field of the unsubstituted ring.

The broad transferability of substituent effects in $\pi$-stacking interactions provides new insight into their origin, with important implications for qualitative models of these effects. First, the correlation of substituent effects in sandwich dimers in which the unsubstituted ring is unchanged bolsters the local, direct interaction model of substituent effects in $\pi$-stacking interactions.[14] Moreover, the existence of additional correlations between substituent effects in diverse stacked dimers revealed that the local, direct interaction model is a special case of a broader understanding of substituent effects in $\pi$-stacking interactions based on the electric fields of the unsubstituted rings.

However, we note here that the above results are for highly constrained model dimers in which the stacked rings are perfectly aligned, and perfectly parallel. Such arrangements are rare in molecular systems, although they do occur.[39] As such, the observed trends might not be fully applicable to more common, parallel-displaced configurations. In particular, the unexpected correlations between substituent effects in diverse stacked dimers are in part due to coincidental similarities of the electric fields above benzene and borazine. Regardless, that substituent effect trends in these model dimers can be explained in terms of electric fields provides a potentially powerful tool for analyzing substituent effects in $\pi$-stacking interactions. For example, work by Arnstein and Sherrill[34] revealed that substituent effects in parallel-displaced benzene dimers vary significantly as a function of displacement distance. Although possible qualitative explanations of observed trends were provided in that work, the present results suggest that consideration of electric fields could provide a more-precise explanation. Future analyses of more-diverse systems, in terms of computed electric fields, should move us one step closer to a comprehensive understanding of substituent effects in $\pi$-stacking interactions.

## ■ ASSOCIATED CONTENT

### Ⓢ Supporting Information

Full citation for refs 86, 87, and 88. Additional figures and computational details, interaction energies for individual dimers, SAPT0 components, electronic energies, and Cartesian coordinates. This material is available free of charge via the Internet at http://pubs.acs.org.

## ■ AUTHOR INFORMATION

### Corresponding Author

*E-mail: wheeler@chem.tamu.edu.

### Notes

The authors declare no competing financial interest.

## ■ ACKNOWLEDGMENTS

This work was supported in part by the National Science Foundation (Grant No. CHE-1254897) and we acknowledge the Texas A&M Supercomputing Facility for computational resources. J. S. Siegel and T. Lu are thanked for fruitful discussions.

## REFERENCES


(1) Salonen, L. M.; Ellermann, M.; Diederich, F. *Angew. Chem., Int. Ed.* **2011**, *50*, 4808−4842.
(2) Meyer, E. A.; Castellano, R. K.; Diederich, F. *Angew. Chem., Int. Ed.* **2003**, *42*, 1210−1250.
(3) Schneider, H.-J. *Angew. Chem., Int. Ed.* **2009**, *48*, 3924−3977.
(4) Zürcher, M.; Diederich, F. *J. Org. Chem.* **2008**, *73*, 4345−4361.
(5) Knowles, R. R.; Jacobsen, E. N. *Proc. Natl. Acad. Sci. U.S.A.* **2010**, *107*, 20678−20685.
(6) Takenaka, N.; Chen, J. S.; Captain, B. *Org. Lett.* **2011**, *13*, 1654−1657.
(7) Lu, T.; Zhu, R.; An, Y.; Wheeler, S. E. *J. Am. Chem. Soc.* **2012**, *134*, 3095−3102.
(8) Raju, R. K.; Bloom, J. W. G.; An, Y.; Wheeler, S. E. *ChemPhysChem* **2011**, *12*, 3116−3130.
(9) Hains, A. W.; Liang, Z.; Woodhouse, M. A.; Gregg, B. A. *Chem. Rev.* **2010**, *110*, 6689−6735.
(10) Bassani, D. M.; Jonusauskaite, L.; Lavie-Cambot, A.; McClenaghan, N. D.; Pozzo, J.-L.; Ray, D.; Vives, G. *Coord. Chem. Rev.* **2010**, *254*, 2429−2445.
(11) Wheeler, S. E. *CrystEngComm* **2012**, *14*, 6140−6145.
(12) Sherrill, C. D. In *Reviews in Computational Chemistry*; Lipkowitz, K. B., Cundari, T. R., Eds.; Wiley−VCH: New York, 2009; Vol. *26*, pp 1−38.
(13) Sinnokrot, M. O.; Valeev, E. F.; Sherrill, C. D. *J. Am. Chem. Soc.* **2002**, *124*, 10887−10893.
(14) Wheeler, S. E. *J. Am. Chem. Soc.* **2011**, *133*, 10262−10274.
(15) Wheeler, S. E. *Acc. Chem. Res.* **2013**, *46*, 1029−1038.
(16) Hohenstein, E. G.; Duan, J.; Sherrill, C. D. *J. Am. Chem. Soc.* **2011**, *133*, 13244−13247.
(17) Watt, M.; Hardebeck, L. K. E.; Kirkpatrick, C. C.; Lewis, M. *J. Am. Chem. Soc.* **2011**, *133*, 3854−3862.
(18) Hunter, C. A.; Sanders, J. K. M. *J. Am. Chem. Soc.* **1990**, *112*, 5525−5534.
(19) Hunter, C. A.; Lawson, K. R.; Perkins, J.; Urch, C. J. *J. Chem. Soc., Perkins Trans. 2* **2001**, 651−669.
(20) Cockroft, S. L.; Hunter, C. A.; Lawson, K. R.; Perkins, J.; Urch, C., J. *J. Am. Chem. Soc.* **2005**, *127*, 8594−8595.
(21) Cockroft, S. L.; Hunter, C. A. *Chem. Soc. Rev.* **2007**, *36*, 172−188.
(22) Cockroft, S. L.; et al. *Org. Biomol. Chem.* **2007**, *5*, 1062−1080.
(23) Cozzi, F.; Cinquini, M.; Annunziata, R.; Dwyer, T.; Siegel, J. S. *J. Am. Chem. Soc.* **1992**, *114*, 5729−5733.
(24) Cozzi, F.; Cinquini, M.; Annunziata, R.; Siegel, J. S. *J. Am. Chem. Soc.* **1993**, *115*, 5330−5331.
(25) Cozzi, F.; Ponzini, F.; Annunziata, R.; Cinquini, M.; Siegel, J. S. *Angew. Chem., Int. Ed.* **1995**, *34*, 1019−1020.
(26) Cozzi, F.; Siegel, J. S. *Pure Appl. Chem.* **1995**, *67*, 683−689.
(27) Cozzi, F.; Annunziata, R.; Benaglia, M.; Cinquini, M.; Raimondi, L.; Baldridge, K. K.; Siegel, J. S. *Org. Biomol. Chem.* **2003**, *1*, 157−162.
(28) Cozzi, F.; Annunziata, R.; Benaglia, M.; Baldridge, K. K.; Aguirre, G.; Estrada, J.; Sritana-Anant, Y.; Siegel, J. S. *Phys. Chem. Chem. Phys.* **2008**, *10*, 2686−2694.
(29) Sinnokrot, M. O.; Sherrill, C. D. *J. Phys. Chem. A* **2003**, *107*, 8377−8379.
(30) Sinnokrot, M. O.; Sherrill, C. D. *J. Am. Chem. Soc.* **2004**, *126*, 7690−7697.
(31) Ringer, A. L.; Sinnokrot, M. O.; Lively, R. P.; Sherrill, C. D. *Chem.—Eur. J.* **2006**, *12*, 3821−3828.
(32) Lee, E. C.; Kim, D.; Jurečka, P.; Tarakeshwar, P.; Hobza, P.; Kim, K. S. *J. Phys. Chem. A* **2007**, *111*, 3446−3457.
(33) Wheeler, S. E.; Houk, K. N. *J. Am. Chem. Soc.* **2008**, *130*, 10854−10855.
(34) Arnstein, S. A.; Sherrill, C. D. *Phys. Chem. Chem. Phys.* **2008**, *10*, 2646−2655.
(35) Wheeler, S. E.; Houk, K. N. *J. Chem. Theory Comput.* **2009**, *5*, 2301−2312.
(36) Wheeler, S. E.; Houk, K. N. *Mol. Phys.* **2009**, *107*, 749−760.
(37) Ringer, A. L.; Sherrill, C. D. *J. Am. Chem. Soc.* **2009**, *131*, 4574−4575.
(38) Seo, J.-I.; Kim, I.; Lee, Y. S. *Chem. Phys. Lett.* **2009**, *474*, 101−106.
(39) Wheeler, S. E.; McNeil, A. J.; Müller, P.; Swager, T. M.; Houk, K. N. *J. Am. Chem. Soc.* **2010**, *132*, 3304−3311.
(40) Rashkin, M. J.; Waters, M. L. *J. Am. Chem. Soc.* **2002**, *124*, 1860−1861.
(41) Sham, I. H. T.; Kwok, C.-C.; Che, C.-M.; Zhu, N. *Chem. Commun.* **2005**, 3547−3549.
(42) Yamaguchi, S.; Wakamiya, A. *Pure Appl. Chem.* **2006**, *78*, 1413−1424.
(43) Anthony, J. E. *Chem. Rev.* **2006**, *106*, 5028−5048.
(44) Bunz, U. H. F. *Chem.—Eur. J.* **2009**, *15*, 6780−6789.
(45) Bunz, U. H. F. *Pure Appl. Chem.* **2010**, *82*, 953−968.
(46) Bunz, U. H. F.; Engelhart, J. U.; Lindner, B. D.; Schaffroth, M. *Angew. Chem., Int. Ed.* **2013**, *52*, 3810−3821.
(47) Zhong, H.; Lai, H.; Fang, Q. *J. Phys. Chem. C* **2010**, *115*, 2423−2427.
(48) Luechai, A.; Gasiorowski, J.; Petsom, A.; Neugebauer, H.; Sariciftci, N. S.; Thamyongkit, P. *J. Mater. Chem.* **2012**, *22*, 23030−23037.
(49) Kuhn, P.; Antonietti, M.; Thomas, A. *Angew. Chem., Int. Ed.* **2008**, *47*, 3450−3453.
(50) Jackson, K. T.; Rabbani, M. G.; Reich, T. E.; El-Kaderi, H. M. *Polym. Chem.* **2011**, *2*, 2775−2777.
(51) Reich, T. E.; Jackson, K. T.; Jena, P.; El-Kaderi, H. M. *J. Mater. Chem.* **2011**, 10629−10632.
(52) Reich, T. E.; Behera, S.; Jackson, K. T.; Jena, P.; El-Kaderi, H. M. *J. Mater. Chem.* **2012**, *22*, 13524−13528.
(53) Jackson, K. T.; Reich, T. E.; El-Kaderi, H. M. *Chem. Commun.* **2012**, *48*, 8823−8825.
(54) Luo, W.; Neiner, D.; Karkamkar, A.; Parab, K.; Garner, E. B.; Dixon, D. A.; Matson, D.; Autrey, T.; Liu, S.-Y. *Dalton Trans.* **2013**, *42*, 611−614.
(55) Luo, W.; Campbell, P. G.; Zakharov, L. N.; Liu, S.-Y. *J. Am. Chem. Soc.* **2011**, *133*, 19326−19329.
(56) Campbell, P. G.; Zakharov, L. N.; Grant, D.; Dixon, D. A.; Liu, S.-Y. *J. Am. Chem. Soc.* **2010**, *132*, 3289−3291.
(57) Abbey, E. R.; Liu, S.-Y. *Org. Biomol. Chem.* **2013**, *11*, 2060−2069.
(58) Knack, D. H.; Marshall, J. L.; Harlow, G. P.; Dudzik, A.; Szaleniec, M.; Liu, S.-Y.; Heider, J. *Angew. Chem., Int. Ed.* **2013**, *52*, 2599−2601.
(59) Campbell, P. G.; Marwitz, A. J. V.; Liu, S.-Y. *Angew. Chem., Int. Ed.* **2012**, *51*, 6074−6092.
(60) Liu, L.; Marwitz, A. J. V.; Matthews, B. W.; Liu, S.-Y. *Angew. Chem., Int. Ed.* **2009**, *48*, 6817−6819.
(61) Anand, B.; Nöth, H.; Schwenk-Kircher, H.; Troll, A. *Eur. J. Inorg. Chem.* **2008**, *2008*, 3186−3199.
(62) Kawahara, S.; Tsuzuki, S.; Uchimaru, T. *J. Chem. Phys.* **2003**, *119*, 10081−10087.
(63) Bettinger, H. F.; Kar, T.; Sánchez-García, E. *J. Phys. Chem. A* **2009**, *113*, 3353−3359.
(64) Ugozzoli, F.; Massera, C. *CrystEngComm* **2005**, *7*, 121−128.
(65) Bates, D. M.; Anderson, J. A.; Oloyede, P.; Tschumper, G. S. *Phys. Chem. Chem. Phys.* **2008**, *10*, 2775−2779.
(66) Wang, W.; Hobza, P. *ChemPhysChem* **2008**, *9*, 1003−1009.
(67) Mishra, B. K.; Arey, J. S.; Sathyamurthy, N. *J. Phys. Chem. A* **2010**, *114*, 9606−9616.
(68) Guin, M.; Patwari, G. N.; Karthikeyan, S.; Kim, K. S. *Phys. Chem. Chem. Phys.* **2011**, *13*, 5514−5525.
(69) Guin, M.; Patwari, G. N.; Karthikeyan, S.; Kim, K. S. *Phys. Chem. Chem. Phys.* **2009**, *11*, 11207−11212.
(70) Sütay, B.; Tekin, A.; Yurtsever, M. *Theor. Chem. Acc.* **2012**, *131*, 1120.
(71) Hampel, C.; Peterson, K. A.; Werner, H.-J. *Chem. Phys. Lett.* **1992**, *190*, 1−12.

(72) Raghavachari, K.; Trucks, G. W.; Pople, J. A.; Head-Gordon, M. *Chem. Phys. Lett.* **1989**, *157*, 479−483.
(73) Jeziorski, B.; Moszyński, R.; Szalewicz, K. *Chem. Rev.* **1994**, *94*, 1887−1930.
(74) Szalewicz, K. *WIREs Comput. Mol. Sci.* **2012**, *2*, 254−272.
(75) Hohenstein, E. G.; Sherrill, C. D. *J. Chem. Phys.* **2010**, *133*, 014101.
(76) Hohenstein, E. G.; Sherrill, C. D. *J. Chem. Phys.* **2010**, *132*, 184111.
(77) Schafer, A.; Huber, C.; Ahlrichs, R. *J. Chem. Phys.* **1994**, *100*, 5829−5835.
(78) Dunning, T. H., Jr. *J. Chem. Phys.* **1989**, *90*, 1007−1023.
(79) Grimme, S. *J. Comput. Chem.* **2006**, *27*, 1787−1799.
(80) Becke, A. *J. Chem. Phys.* **1997**, *107*, 8554−8560.
(81) Boys, S. F.; Bernardi, F. *Mol. Phys.* **1970**, *19*, 553−566.
(82) Kendall, R. A.; Dunning, T. H., Jr.; Harrison, R. J. *J. Chem. Phys.* **1992**, *96*, 6796−6806.
(83) Papajak, E.; Truhlar, D. G. *J. Chem. Theory Comput.* **2011**, *7*, 10−18.
(84) Sinnokrot, M. O.; Sherrill, C. D. *J. Phys. Chem. A* **2006**, *110*, 10656−10668.
(85) Pettersen, E. F.; Goddard, T. D.; Huang, C. C.; Couch, G. S.; Greenblatt, D. M.; Meng, E. C.; Ferrin, T. E. *J. Comput. Chem.* **2004**, *25*, 1605−1612.
(86) Frisch, M. J., et al. *Gaussian 09, Revision B.01*; Gaussian, Inc.: Wallingford, CT, 2009.
(87) MOLPRO, version 2010.1, is a package of ab initio programs written by H.-J. Werner, et al.
(88) Turney, J. M.; et al. *WIREs Comput. Mol. Sci.* **2012**, *2*, 556−565.
(89) Fowler, P. W.; Buckingham, A. D. *Chem. Phys. Lett.* **1991**, *176*, 11−18.
(90) Bloom, J. W. G.; Wheeler, S. E. *Angew. Chem., Int. Ed.* **2011**, *50*, 7847−7849.
(91) Islas, R.; Chamorro, E.; Robles, J.; Heine, T.; Santos, J. C.; Merino, G. *Struct. Chem.* **2007**, *18*, 833−839.
(92) Bloom, J. W. G.; Raju, R. K.; Wheeler, S. E. *J. Chem. Theory Comput.* **2012**, *8*, 3167−3174.
(93) The unsubstituted ring can alter the substituent effects in an indirect way, for example, by altering the inter-ring separation of the dimer.